2015

Tree-Sway Frequency And The Turbulent Co-Spectral Gap In A Dense Canopy Environment

Katherine L. Ertell
University of South Carolina

TREE-SWAY FREQUENCY AND THE TURBULENT CO-SPECTRAL GAP IN A DENSE CANOPY ENVIRONMENT

By

Katherine L Ertell

Bachelor of Science
Valparaiso University, 2012

Submitted in Partial Fulfillment of the Requirements

For the Degree of Master of Science in

Geography

College of Arts and Sciences

University of South Carolina

2015

Accepted by:

April Hiscox, Director of Thesis

Greg Carbone, Reader

Sarah Battersby, Reader

Lacy Ford, Vice Provost and Dean of Graduate Studies

ACKNOWLEDGEMENTS

Thank you to my wonderful family—Mom, Dad and Andy—for your endless support for my crazy dreams and passions that have now turned into a career that I love and look forward to each and every day. I could not have done it without your direction. You all truly are the best role models I could have ever asked for.

Thank you to my wonderful Graduate Advisor, Dr. April Hiscox, for your constant encouragement and patience as I juggled moving far from home and getting my first job all in the last two years. I could not have accomplished this without your guidance.

Thank you to my readers, Greg Carbone and Sarah Battersby, for sharing your expertise and helpful feedback in this project.

Thank you to my undergraduate professors at Valparaiso University, Dr. Teresa Bals-Elsholz and Dr. Bharath Ganesh-Babu, who pushed me to pursue my Masters degree at the University of South Carolina and helped me to find my niche in the field of Meteorology and GIS.

ABSTRACT

Today, knowledge of canopy turbulence comes solely from field observations. However, measurements or field observations that are taken at a specific location within the canopy cannot accurately capture the interaction of the wind and the canopy it crosses. Without this complete picture of the atmosphere, the temporal fluctuations that exist in turbulent flows cannot be understood. From an atmospheric perspective, the complex structure of forests significantly influences turbulence in the atmospheric boundary layers (ABL) by consistently imposing both mechanical and thermal forces. This study explores the temporal and spatial characteristics of tree-sway motions and their aerodynamic interactions with coherent turbulence wind fields in a forest (Howland Forest, ME). Flux calculations from tower data, such as in this experiment, require the researcher to choose a timescale to define fluctuations, however since the atmosphere typically contains motions and coherent vertical transports on a multitude of timescales; the selection of it is not always straightforward. This study will aid in answering whether or not there is a correlation between average stem sway frequency and the turbulent co-spectral gap in a forest environment. Results were achieved by using a multi-resolution decomposition (MRD) technique to find a day-time specific time scale and then examining the tree's frequencies at that time scale through a Fourier transform to determine if MRD can find an appropriate time scale of coherent motions. Through a mapping comparison, the sub-mesoscale motions of a canopy atmosphere and their effect on the tree's movement as well as fluxes of energy were better understood. Less

coherence was seen when examining motion on time scales greater than the co-spectral gap, which would include meso and sub meso scale motions. Frequency proved to be a good variable for mapping the wind. Overall this work highlights the usefulness of dynamic maps for displaying data and better understanding rapidly changing spatial patterns that may have been missed otherwise. This will eventually lead to incorporating canopy motion physics into bigger climate models, as well as providing an explanation to the uneven calculations of many natural cycles, such as the carbon flux cycle.

TABLE OF CONTENTS

List of Figures

LIST OF SYMBOLS

$L_s = U_h/(\partial U/\partial z)_h$	VERTICAL LENGTH SCALE
h	CANOPY HEIGHT
T_S	SONIC TEMPERATURE
u, v, w	WIND COMPONENT
u'w'	VERTICAL KINEMATIC TURBULENT FLUX DENSITY OF THE X-DIRECTION (STREAMWISE) MEAN MOMENTUM (PU)

List of Abbreviations

ABL ..... Atmospheric Boundary Layer

ASL ..... Atmospheric Surface Layer

CRSL ..... Canopy Roughness Sublayer

FFT ..... Fast Fourier Transform

IDW ..... Inverse Distance Weighting

MOST ..... Monin–Obukhov Similarity Theory

MR ..... Multiresolution

MRD ..... Multi-Resolutional Decomposition

PML ..... Plane Mixing Layer

CHAPTER 1: INTRODUCTION

Wind flow within forest canopies is important for studies of atmospheric waves (Lee and Barr, 1997) and turbulence exchange (Finnigan, 2000). In the boundary layer, transport of quantities such as moisture, heat, momentum, and pollutants is dominated in the horizontal direction by the mean wind and in the vertical direction by turbulence. Turbulent winds drive scalar dispersion and exchanges of heat and mass between plants and their surrounding atmospheric environment (Moneith, 1981). These exchange processes and their influences on the physiological functions of terrestrial plants continue to be significant components of global hydrological and carbon cycles (Monsi et al., 1973, Baldocchi et al., 2002, Law et al., 2002).

More than a third of the Earth's surface is covered by vegetation. Vegetation repeatedly influences the climate through the exchanges of energy, water, carbon dioxide, and other chemicals found in the atmosphere. These particular exchanges and their associated wind transport aid in furthering the accuracy of climate models today. However, understanding and quantitatively analyzing the wind flow in the lowest section of the boundary layer becomes even more complex due to the inherent thermal and mechanical influence of the canopy elements (Raupach et al., 1996). Understanding the processes driving vegetation–atmosphere exchange would aid in a clearer understanding of weather, climate, and environmental forecasting as well as a further advancement in

problems which arise in agricultural and natural resource management, including catastrophic wind damages to crops and forests (Foster and Boose, 1992).

Forest ecosystems are structurally more complex, and live much longer than agricultural crops. They therefore continuously adapt to local wind conditions over many years. The susceptibility of a forest canopy to wind forces is strongly linked to not only its structure (Canham and Loucks 1984) but also its thigmic response to wind induced bending stresses (Telewski and Pruyn 1998, Henry and Thomas 2002). Investigations into the relationship between forest canopy structures and their thigmic responses to local wind regimes are only in their infancy (Rudnicki et al. 2004). Catastrophic windstorms at a landscape scale (Boose et al. 1994) are predicted to increase the frequency and size of forest disturbances in the near future (Peterson 2000). Even with that pressing knowledge, uncertainties remain regarding the interactions between changing forest disturbance dynamics and predicted climate change patterns. (Dale et al. 2001). A mechanistic understanding of the dynamics of individual tree stability and failure (Baker 1995, James et al. 2006) is critical to predict how forest structures and functions (e.g., succession) would respond to future global environmental changes, in particular more frequent and stronger windstorms—before they occur (Emanuel 2005, Trapp et al. 2007).

From an atmospheric perspective, the dynamic and complex construction of forested ecosystems has significant influences on turbulence structures in the atmospheric boundary layers (ABL). A forest canopy consistently imposes energy in both mechanical and thermal forces. The lower layer of the atmosphere responds directly to changes in surface fluxes of momentum, energy, and other scalars, typically on a timescale of about

an hour or less. Examples of these forces or changes that can influence the ABL are: frictional drag, evaporation and transpiration, heat transfer, pollutant emission, and terrain induced flow modification.

In Roland Stoll's *An Introduction to Boundary Layer Meteorology* (1988), he explains that wind in the boundary layer can be divided into three categories: mean wind, turbulence, and waves. Each can exist separately, or in presence of any others within the boundary layer of the atmosphere. Mean wind, often connected to advection, is characterized as very rapid horizontal transport. Rapid horizontal winds on the order of 2 to 10m/s are often found in the ABL. Turbulent fluxes can be defined loosely as the collection of links between random fluctuations in velocity and scalars that effectively transport energy from the Earth's surface into the troposphere. Waves are winds that transport little heat, humidity, and other scalars, but effectively transport momentum and energy. Waves can serve as an initiator of turbulence as they often cause enhanced wind shears in localized regions. In the boundary layer, unlike the rest of the atmosphere, there is an abundance of turbulence near the surface. In the canopy roughness sublayer (CRSL) (Kaimal and Finnigan 1994), a layer that extends upward from z=h (vertical=canopy height) to about 2h (twice the canopy height), turbulence characteristics, momentum transfer, and the transport, diffusion and deposition of scalars and particles are strongly influenced by canopy morphology.

In the lowest 10% of the ABL, called the "atmospheric surface layer" (ASL), a series of assumptions are made to describe turbulent wind behavior. We may assume that in turbulent flow the actual flow velocity is equal to the average velocity V plus the

fluctuating turbulent velocities U,v,w in the x,y,z directions, respectively. The term U'w', the vertical kinematic turbulent flux density of the x-direction (streamwise) can be used to show turbulence in the ASL. When the ASL is turbulent, then U′w′ will be constant with height. The assumption of a constant vertical flux allows the use of these constant fluxes as parameters in a set of relationships known as Monin–Obukhov Similarity Theory (MOST). Work over the last several years by Patton and Finnigan (2009), and Vickers and Mahrt (2002), has shown that MOST is not always applicable, particularly at night in canopies.

Under these conditions, the downward turbulent momentum flux u′w′ continually decreases. This is can be attributed to that mean streamwise momentum (ρu), which is the momentum absorbed through the aerodynamic drag on the plants. Therefore, within the canopy, the similarity scaling leading to the log-law and MOST is no longer applicable. This means that there is not a direct connection between scalar turbulent fluxes and scalar local gradients. A basic understanding of the nature of canopy turbulence can make this difference more clear.

Turbulence, the gustiness superimposed on the mean wind, can be visualized as consisting of irregular swirls or motion called eddies. Turbulence can also be thought of as a collection of many different sized eddies all superimposed on each other. The turbulence spectrum is therefore made up of the relative strength of these different scale eddies. Almost all of the boundary layer turbulence is caused or generated by forcings from the earth's surface. An example of this is solar heating. On sunny days, the ground heats up. This causes pockets of warmer air to rise. These pockets, or thermals can be

classified as large scale eddies. Obstacles such as trees and buildings affect the flow by deflecting it, causing turbulent wakes adjacent to, but downwind from an obstacle.

Information on the size of eddies and on the scale of motions in the boundary layer is needed to understand turbulence. Unfortunately, capturing a snap shot picture of the ABL is not an easy task. Canopy sized turbulent eddies have been reported in previous studies (Raupach, Finnigan et al. 1996), however, the turbulent eddies-- which are influenced by the motion of the canopy elements-- remain poorly explored due to lack of detailed understanding of tree motions. Improved understanding of turbulence structures and modeling of turbulent transport and diffusion in the CRSL are needed to understand the flux exchanges within and above a canopy (Gardiner, 1995).

When questions of plant canopy turbulence first appeared, researchers assumed it could be treated like boundary layer turbulence with a few additions of fine scale eddies that were generated by obstacles. By the 1970s, it had become clear that the dominant eddies in plant canopy turbulent flows are much larger than the added plant element size researchers had considered. After discovering that the addition would not account for the difference, it took more than two decades of research to account for the generated canopy drag that is caused by the plant elements rather than as friction on the ground (Finnigan, 2000).

However, it wasn't just as simple as incorporating canopy drag. The distribution of mean velocity in the canopy air is not only due to canopy drag, but instead is the result of the interaction between the downward turbulent transport of momentum and canopy drag.

Canopy drag varies with height and depends on both the foliage distribution as well as the velocity field itself in a particular forest or terrain. Similarly, the within-canopy distribution of scalar concentrations results from a balance between turbulent transfer and the distribution of scalar sources and sinks. As Patton and Finnigan note (2012), the location of these scalar sources/ sinks are determined by three factors: (1) solar radiation as it filters through the foliage, (2) the biological state of the plants such as their access to soil water, and (3) the ambient concentrations of temperature, humidity, CO2, and other scalars in the canopy airspace. Recent research (Rudnicki, 2004) also suggests that the motion of canopy elements may also play a role, although this is difficult to measure.

To fully understand spatial wind fields, it would be necessary to take measurements at many locations. This is often not possible and it is easier to make measurements at one point in space over a long period of time. In 1938, G. I. Taylor suggested that, "for some special cases, turbulence can be considered to be frozen as it advects past a sensor. Thus, the wind speed could be used to translate turbulence measurements as a function of time to their corresponding measurements in space." However, Powel and Elderkin pointed out in 1974 that "turbulence is not really "frozen" and Taylor's simplification is thus useful only for those cases where the turbulent eddies evolve with a timescale longer than the time it take the eddy to be advected past a sensor."

Raupach and Thom (1981) state that second-order closure models provide the best hope to replace local-diffusion theory which is seriously deficient in the canopy, and that it may prove possible to incorporate aeroelasticity of plants into these models. However,

the majority of ensemble average models at various orders of closure for airflow in the CRSL (Wilson and Shaw 1977, Katul et al. 2004) do not consider plant motions. It is currently unclear how much of the reported discrepancies between measured and modeled velocity variances near the canopy top (Wilson and Shaw 1977) could be due to ignoring plant waving in these models.

Experimental findings later underscore the importance of modeling wind-driven plant motion. Finnigan and Mulhearn (1978) argued:

> *"Although the motions of individual wheat and barley stalks are excited by a turbulent wind, single stalks vibrate at a particular and well defined natural frequency, which enables them to be treated as resonant cantilevers, whose elastic properties can be measured by well-established engineering techniques".*

The simple model that Finnigan and Mulhearn (1978) developed was able to simulate the influence of vegetation density observed in a wind tunnel experiment indicating that the effect of the waving stalks is seen as a strong peak at the waving frequency in the power spectrum of streamwise velocity fluctuations. This peak is completely absent in the case of a sparse model canopy (Finnigan and Mulhearn, 1978).

Other studies have explored the use of laboratory simulations where much of the turbulence work has been performed in laboratory tanks, usually using a liquid such as water to simulate an environment—or a forest terrain in this case. Although there has been some success in laboratory studies, there have only been a select few that simulate larger phenomena. Wind tunnels have also been used to observe the flow of neutral boundary layers over complex terrain and buildings, however those studies could not

adequately simulate the typical daytime and nighttime boundary layer characteristics. (Finnigan et al, 2009)

One unique approach of handling extreme wind events involves simulations of the dynamic response of trees to the wind. (Lee, 2000). It is recognized that wind damage to trees is most likely to occur at high wind speeds and when the excitation frequency (frequency of wind gusts) coincides with the natural frequency of sway vibrations. The resonance is considered to occur if the spectral peak frequency of the velocity time series matches the natural frequency of sway vibrations (Mayer, 1989; Gardiner, 1994; Wood, 1995; Peltola, 1996).

One of the most striking examples of wind-induced plant motions, which is of most interest in this study, is the honami (in Japanese, "*ho*" = "*cereal*", "*nami*" = "*wave*"), which refers to ocean-wave-like motions of cereal crops on windy days observed over a half century ago. Several field observations (Finnigan and Mulhearn 1978) provided some of the earliest qualitative and quantitative evidences on the significant aerodynamic interactions between waving plants and CRSL turbulence. Analyses of movie films of waving stalks in a barley (Finnigan and Mulhearn 1978) and a wheat field (Finnigan 1979) drew the following picture: when a honami event took place, the crop field was divided into patches of coherent waves with abrupt and arbitrary phase differences between adjacent patches. Individual patches were 15-20h (h is mean stalk height) in downwind extent, 5-6h in the crosswind extent, and retained their identity for about 5 seconds on average. Five distinct crests were seen in any patch so that the wavelength is 3-4h in the streamwise direction. The phase velocity (estimated as the passage velocity of

a crest at a point in space) is 4 (Finnigan and Mulhearn 1978) to 1.8 (Finnigan 1979) times the mean velocity at the canopy top. These spatial and temporal characteristics suggest that honami events are one of the first records of canopy motion that are driven by large coherent wind gusts.

Another, more recent, example is an experiment in a dense spruce forest (Gardiner 1994), which also showed that momentum transport and tree motions are dominated by intermittent sweep/ejection events associated with honami waves moving across the forests. Gardiner's (1994) spectral analysis indicated that trees efficiently absorb energy at the resonant frequency and short-circuit the inertial energy cascade.

A noteworthy theoretical development reviewed in Finnigan (2000) is the proposal by Raupach et al. (1996) that the CRSL is more analogous to a plane-mixing-layer (PML) than a boundary layer as originally believed. This is mainly based on common features observed in both types of flows: an inflection point in the mean velocity profile, similar ratios between components of the Reynolds stress tensor, the relative role of sweeps and ejections, length scales of active turbulence, and that dominant large eddies are the results of an instability in the ABL due to the inflected mean velocity profile. A vertical length scale: $L_s = U_h/(\partial U/\partial z)_h$, where U_h and $(\partial U/\partial z)_h$ are the mean velocity and its vertical gradient at the canopy top, is used to distinguish the inactive ($>> L_s$), active ($\sim L_s$) and fine-scale ($<< L_s$) turbulence. The effect of vegetation density is such that L_s is around 0.1*h*, 0.5*h* and *h* for dense, moderate and sparse canopies. A main effect of the large inactive eddies is to make the active canopy-scale eddies intermittent. Each large-scale

gust initiates a "wave packet" of several canopy-scale coherent eddies with a streamwise separation of $L_x = mL_s$ ($m = 8.1 \pm 0.3$), which varies from instance to instance of large-scale gusts.

However, the PML analogy is incomplete for a CRSL that is embedded in the ABL. There is distinct asymmetry above and below the inflection point near the canopy top. Different interpretations (Finnigan and Shaw 2000, Watanabe 2004) of the relation (interactions, mechanisms) between the large-scale gusts from the outer part of the ABL (Finnigan 1979) and the "wave packet" or train of several canopy-scale eddies (Raupach et al. 1996) remain to be reconciled and fully understood. Interactions between buoyancy forces and "inflectional instability" need to be further investigated. Both earlier (Finnigan and Mulhearn 1978, Finnigan 1979) and more recent (Py et al. 2005) experiments in and above short crops observed that the wavelength of honami waves increases with increasing mean wind speed.

Previous linear models are only a small step towards a full understanding of the canopy wave dynamics because, in reality, shear-generated waves can quickly grow out of the linear phase. One feature evident of almost all canopy wave events is the existence of a monochromatic wave frequency.

A key factor of the equation is still missing. Although oscillations of free-swaying plants and trees have been explored (Mayer 1987, Milne 1991, Gardiner 1992, Speck and Spatz 2004), tree sway within a dense forest remains poorly understood. This is primarily due to complex sway damping factors (Milne 1991, Rudnicki et al. 2008) and the

difficulty of quantifying group sway (Mayer 1987, Gardiner 1992). More recently, Rudnicki et al. (2008) reported that the sway frequency for a group of slender trees (experiencing many intense crown collisions) decreases with increasing wind speed but did not change for a group of stout trees (experiencing few and light collisions), and that collisions between adjacent trees enhance damping and reduce sway energy. Previous work at this field site has shown that distribution of sway frequency over the canopy closely matched the associated spatial distribution of slenderness. (Rudnicki, Personal Communication)

Modeling a forest canopy flow under very stable conditions (intermittent turbulence regime) is a challenging task. (Lee, 2000). The prominent problem arises from the difficulty in finding an interval suitable for performing the Reynolds averaging when the turbulence is globally intermittent (Mahrt, 1999). Because static stability plays an important part in the flow dynamics, a successful model must include a proper parameterization of the heat exchange between the air and the plants. Mahrt et al. (2001) discovered a spectral gap, which delineated turbulence and mesoscale motions by examining what is known as the multi-resolution (MR) spectra (variances) of the wind components for a variety of different tower datasets. This spectral gap is the key to understanding the dynamic atmosphere of a forest environment.

OBJECTIVES

A large hole exists between forest meteorology studies-- which traditionally are concerned with microscale processes (about 1 km)-- and everyday mesoscale meteorology studies, which are concerned with atmospheric phenomena at scales of

several tens of kilometers. In principle, mesoscale flow models are the desirable tool for studies of wind and turbulence in complex terrain, but the cost of running such models for wind damage assessment is prohibiting. With such a large variety of scales involved in a complex terrain of a forest and the tremendous variability in the vertical element of a canopy a large array of sensors including airborne platforms and remote sensors would be required to understand all the motions in a forest canopy. The relatively large costs have limited the scope of many field experiments and only a few general-purpose, large scales boundary layer experiments have been conducted. (Finnigan et al, 2009) Therefore, it remains an open question whether the mesoscale models can generate accurate wind fields near the tree canopy (Lee, 2000).

This work examines the temporal and spatial characteristics of tree-sway motions and their aerodynamic interactions with coherent turbulence wind fields in a forest. These steps are aimed to answer my hypothesis that there is a correlation between average (or local) sway frequency and the turbulent co-spectral gap in a forest environment.

1) Test the hypothesis by using a multi-resolution decomposition technique to find a night-time specific time scale and then.
2) Examine the tree's fundamental peak frequencies at that time scale through a Fourier transform.
3) Determine if this is a successful way of finding representing the scale of coherent motions which occur in the boundary layer of the atmosphere.
4) Dynamic map frequency changes of trees to identify coherent atmospheric motions.

The focus of this particular project will be to further investigate the aerodynamic interactions between tree sway motions and CRSL wave turbulence in and above a relatively horizontal homogeneous forest in flat terrain.

CHAPTER 2: METHODS

DATA:

All wind and tree-sway data used in this research project were collected at the Howland Forest in Maine, USA, approximately 35 miles north of Bangor (45.238◦ N–68.664◦ W, elevation of 48 m). It is the site of an AMERIFLUX tower as well as a number of other instruments (Hollinger et al., 1999). The topography of the site is very flat with a long and uniform fetch. The region is categorized as Acadian plain and lies in the Penobscot River flood plain. The site is a relatively, evenly aged stand of old growth trees, approximately 130 years old, with a species mix dominated by red spruce and eastern hemlock. The study area is a circle with a diameter of 150m. All trees within the study area with a diameter at breast height (DBH) greater than 10 cm were tagged; and their species, tag number, and DBH were recorded. A total of 1615 trees were included in the survey. The trees' horizontal and vertical positions were measured relative to a site datum using a Leica (TCR 307) total station and recorded with a Trimble data logger running Survey Pro software (Tripod Data Systems). Tree height was measured using an Impulse Laser Rangefinder (Laser Technology Inc., Centennial, CO) and the average canopy height in the measurement area is 20.6 meters. Using a nominal grid spacing of 10 meters, the dominant or co-dominant tree in each grid was instrumented with a clinometer to measure tree stem displacement. *Figure 2.1* shows a computer-generated model of the instrumented trees based on tree height, species and crown measurements.

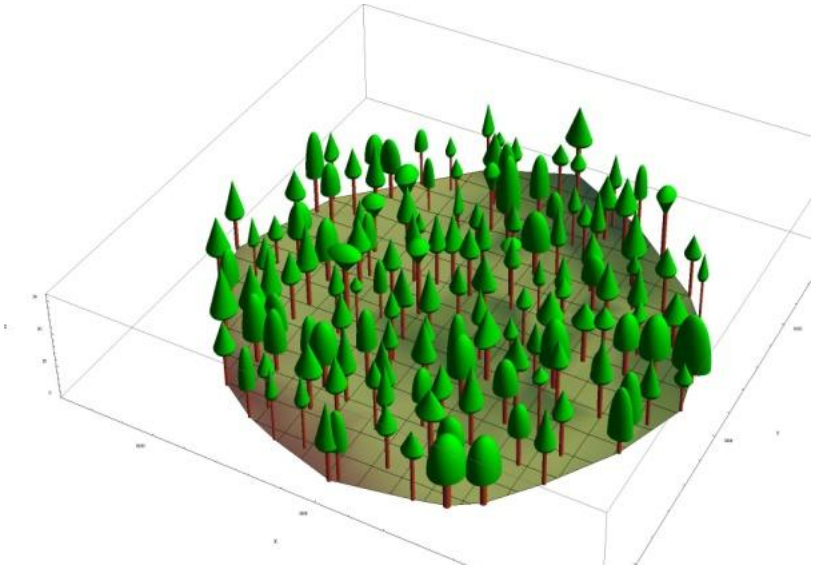

Figure 2.1*: A computer generated model of the instrumented trees based on tree height, species and crown measurements.(Courtesy of M. Rudnicki, The University of Connecticut)*

This work is part of a larger study designed to understand the interactions between tree sway and turbulence in the canopy (Granucci et al., 2013). The tower arrangement was chosen based on the predominant wind flow from west to east seen at the site and shown in the wind rose in *Figure 2.2.*

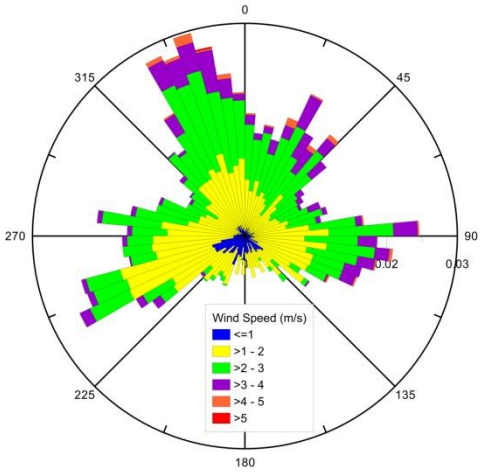

Figure 2.2: *Wind direction distribution for 30-minute averages of winds measured above canopy during daytime convective conditions.*

Each tower at the site was equipped with three CSAT3 sonic anemometers (Campbell Scientific, Inc., Logan, Utah). Each component of the wind speed (u, v, w) and sonic temperature (T_S) was sampled at 10Hz. For this work, data from the central tower was utilized. The anemometers were mounted at heights of 21.4m, 15.1m, and 8.0m on a 27.5m tall, triangle frame tower (Model 25G, Rohn, Peoria, IL). The top anemometer was mounted just above the canopy, within the CRSL. The middle anemometer was placed near the center of the live crown and the bottom was mounted just below the live crown. All anemometers were mounted pointing north. Instruments were operated nearly continuously from August of 2009 to December 2011.

Tree sway on the site was measured using biaxial clinometers (Model 900, Applied Geomechanics) mounted just below the live crown height, an approximate height of 10.1m. Each clinometer was gravity referenced, had a measurement range of ±25◦, a resonant frequency of 10 Hz, and an angular resolution of 0.01◦. Biaxial clinometers are

ideal for tree sway measurement because their response time is much faster than tree sway velocities and they were easily attached to the tree's stem. A total of 149 trees were equipped with clinometers. Clinometer data was stored as raw voltage values and converted to displacement values in meters using calibrations for each individual sensor.

DATA ANALYSIS

To test the hypothesis, the collected data went through several analysis steps. The first of these steps was to use the turbulent wind measurements to identify a potential gust frequency time step. The appropriate time step, which was determined by the MRD method (Vickers and Marht, 1997), depends on the average wind speed of each particular night, and therefore cannot be satisfied with a generic timescale for the entirety of the experiment, like many researchers have assumed before (Raupach, 1989; Shaw, 1992). Once the corresponding time step was determined, that period was used to find the change in the fundamental peak frequency of each individual tree over the course of the night. The fundamental peak frequency of each tree was found by using the Fast Fourier Transform Method. Performing a Fast Fourier Transform on each individual tree gives a picture of the universal motion of the trees, at the predetermined time scale, throughout the forest. The changes in the determined peak frequencies were then dynamically mapped to help identify coherent structures—proposed at the predetermined time scale. For comparison, the FFT was also be performed on a timescale double of that found by the MRD, the resulting dynamic maps were compared to the original maps. For this work a visual comparison was used to identify coherency. A more quantitative analysis is the subject of future research. If the hypothesis is correct, the dynamic maps created at

the gap-scale time step will show that the data revealed more coherencies in tree motion than those at the longer timescale.

A. DATA PRE-PROCESSING

Prior to analysis for this experiment, the angular tree sway data were normalized and converted to displacement in order to assess the quality of the data in meters. Data sets were normalized to a zero resting position by identifying an eight hour time period with very low winds speeds (average 0.23m/s), with this average angle subtracted from the data sets used in the analysis. Displacement in meters was then calculated from the normalized tilt angle using the equations specified in Rudnicki et al (2001). The x and y displacements were then resolved into a single horizontal displacement of the center of gravity of the live crown. Center of gravity for each tree was assumed to be half the live crown height (Long and Smith, 1992), which was calculated by subtracting the sensor mount height from the total tree height.

B. DATA SELECTION

Since the work presented here is exploratory, only a small subset of the data was used. The selection was made primarily on the time of day as well as the season (keeping in mind snow covered trees). During the daytime the atmosphere is very unstable which makes the majority of wind events smaller and not as widespread. Unstable air gives way to rising motion and rising motion will affect heat fluxes, causing wind events to be more spread out vertically rather than horizontally during the night. Also, in the evening the boundary layer of the atmosphere suppresses and shrinking vertically, making any events

that linger over night elongated and therefore condensing all of the associated energy into a smaller and long time scale. For this reason, the events should be more recognizable at night. Also, as a result of the nocturnal jet, the turbulence found at nighttime in the static boundary layer sometimes occurs in relatively short bursts and can cause mixing throughout the entire layer.

Vickers and Mahrt (2001) speculated that:

"When relating these fluxes to the local mean wind shear and temperature stratification, as in similarity theory, the prescribed timescale would ideally include transports on all turbulence timescales and exclude all mesoscale and larger motions. Mesoscale motions do not obey similarity theory and are poorly sampled on time scales of a few hours or less. Including mesoscale transport in calculated fluxes potentially degrades similarity relationships (Smedman 1988). This degradation is expected to be most significant for stable conditions, where the turbulent fluxes are small and inclusion of the mesoscale contribution can dramatically change the magnitude and even the sign of the calculated flux. In unstable conditions the turbulent flux is much larger, and therefore inadvertent inclusion of mesoscale transport is thought to have less impact on the calculated flux."

This lead this project to look more closely at nighttime data, rather than daytime, so that there is a better change of "catching" some of the elongated eddies events that enter the study area and pass by the towers.

Typically, these eddies are categorized best in high wind speed events, but for purposes of this study we want to make sure to reduce the miscellaneous changes in fundamental frequencies that may have been brought on by collisions in the upper canopy. Without a collision factor we would ideally use high wind speed days, but will use moderate wind speed days in hopes of catching coherency, but eliminating the collision interference.

Given these criteria two nights were selected for analysis. Both were chosen for the moderate average wind speeds following previous studies, which suggested eddies were more visible when winds were higher and/or more turbulent. Thirty minutes averages of horizontal wind speed, U, were examined for the entire study period. Two nights were chosen based on sustained winds greater than 1.5m/s. These two nights were May 27, 2011, which had an average wind speed of 3m/s and May 30, 2011, which had an average wind speed of 2.4m/s.

C. IDENTIFICATION OF TIME SCALE

Flux calculations from tower data require the researcher to choose a timescale to define the fluctuations. The calculated flux includes all scales of motion from the smallest resolved by the instrumentation up to the specified averaging timescale, and therefore, the calculated flux depends on the choice of the research. Differences in a selection of a timescale may contribute to some of the differences between studies, especially for the stable boundary layer. For example, while studying similarity relationships, one might attempt to remove all non-turbulent contributions to the fluxes, while for balancing surface energy budgets one might want to include heat fluxes at larger timescales, regardless of their origins. Since the atmosphere typically contains motions and coherent vertical transports (fluxes) on a wide range of timescales, the selection of it is not always straightforward. The choice of timescale for finding a

cospectral gap varies in the literature, where a typical value is ~30-40 seconds. (Vickers and Mahrt, 1997)

The scale dependence of the flux often reveals a cospectral gap region that separates the turbulent scales of the cospectra from the mesoscale transport (Smedman and Hogstrom 1975; Stull 1990). These mesoscale flows can include deep convection, large roll vortices and local circulations due to topographical or surface heterogeneity. In stable flows, mesoscale motions can include internal gravity waves, drainage flows, and other less known motions. Wave-turbulence interactions at timescales as small as a few hundred seconds have been observed to cause both gradient and counter gradient heat fluxes in very stable conditions (Smedman 1988; Sun et al. 2002).

When relating fluxes to the local mean wind shear and temperature stratification, as in similarity theory, the prescribed timescale would ideally include transports on all turbulence timescales and exclude all mesoscale and larger motions. Mesoscale motions do not obey similarity theory and are poorly sampled on time scales of a few hours or less (Mahrt et al. 2001). Including mesoscale transport in calculated fluxes potentially degrades similarity relationships (Smedman 1988). This degradation is expected to be most significant for stable conditions, where the turbulent fluxes are small and inclusion of the mesoscale contribution can dramatically change the magnitude and even the sign of the calculated flux. In unstable conditions the turbulent flux is much larger, and therefore inadvertent inclusion of mesoscale transport is thought to have less impact on the calculated flux.

One method of choosing a timescale is Multi-resolution decomposition (MRD) (Vickers and Mahrt, 2006). A multi-resolution decomposition was applied to the raw anemometer data for each night to find the cospectral gap scale-- the timescale that separates turbulent and mesoscale fluxes of heat, moisture, and momentum between the atmosphere and the surface. It is desirable to partition the flux because turbulent fluxes are related to the local wind shear and temperature stratification through similarity theory, while mesoscale fluxes are not. Use of the gap timescale to calculate the eddy correlation flux removes contamination by mesoscale motions, and therefore improves similarity relationships compared to the usual approach of using a constant averaging timescale.

Multiresolution analysis applied to a time series decomposes the record into averages on different time scales and represents the simplest possible orthogonal decomposition. Multiresolution (MR) spectra yield information on the scale dependence of the variance as do Fourier spectra, but unlike Fourier spectra, MR spectra satisfy Reynold's averaging at all scales and do not assume periodicity (Howell and Mahrt 1997). The location of the peak of MR spectra in the time scale domain depends primarily on the timescale of the fluctuations, while the peak of Fourier spectra depends on the periodicity. Howell and Mahrt (1997) found that Fourier spectra tend to be shifted to larger scales because local MR spectra respond to event widths, whereas the global Fourier spectra are influenced by the time between events. Mahrt et al. (2001) found a spectral gap delineating turbulence and mesoscale motions by examining MR spectra (variances) of the wind components for a variety of different tower datasets. We

hypothesize that it is the turbulent scale motions that cause coherent tree motion and therefore that the time scale of the peak MR spectra is the ideal averaging time to determine tree movement frequency.

To objectively find the gap timescale, Vickers and Mahrt developed an automated algorithm. The algorithm scans the MR cospectra beginning with the shortest averaging timescale and progressing to longer timescales. The first peak in the cospectra is identified by a decrease in magnitude with increasing scale and is associated with turbulence. The gap between turbulence and mesoscale motions is identified when the cospectra either increase or level off at an averaging time scale longer than the scale associated with the turbulence peak. A leveling off is identified when the accumulative flux changes by 1% or less with an increase in timescale. For this work the gap was defined as the peak after the first increase. The top sonic anemometer on the two towers serves as a good representation of the entire forest site to find a more ideal integration time. Python code for computing the MRD and identifying the gap scale is included in Appendix A.

Figure 2.3 and 2.4 show the MRD calculated for the two test case days, using data from top anemometers and beginning the calculation one hour after sunset. In *Figure 2.3* the gap is identified as 18.56 seconds. This is the average peak from all five hour segments for the evening. *Figure 2.4* show a longer gap of 53.76 seconds for the second day, May 30, 2011. Each colored line on the graph represents thirty minutes of wind data. The y-axis is the total heat flux cospectra calculated for each time scale. Heat flux, in atmospheric terms is a measure of temperature and vertical wind or essentially a

measure of vertical motion in the atmosphere. Vertical motion in an atmosphere is also another way to think of energy in the atmosphere. It takes energy for air to rise vertically. The x-axis is a time scale measurement on a log scaled axis. The time scale is simply saying that that is the amount of time that it took for an event (eddy) to pass the tower and its associated sonic anemometer. The amount of time essentially is an indicator to the size of an event, and therefore, how much energy the event is possibly holding or moving throughout our forest. These events, especially the ones that occur in the aforementioned gap are affecting the natural fluxes in a forest on a day-to-day basis.

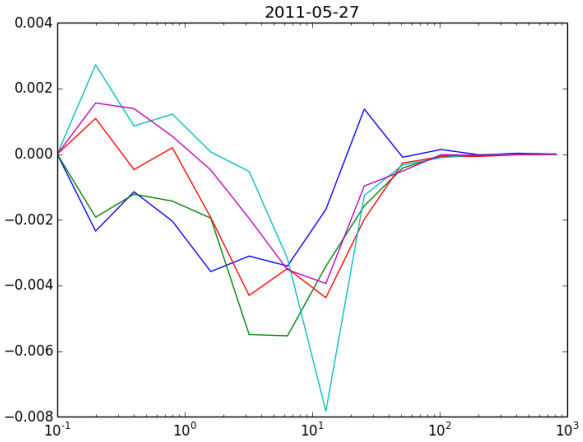

Figure 2.3: *The multi-resolutional decomposition found the gap on May 27, 2011 from 1800-2100. The average of all 5 hours is 18.56 seconds.*

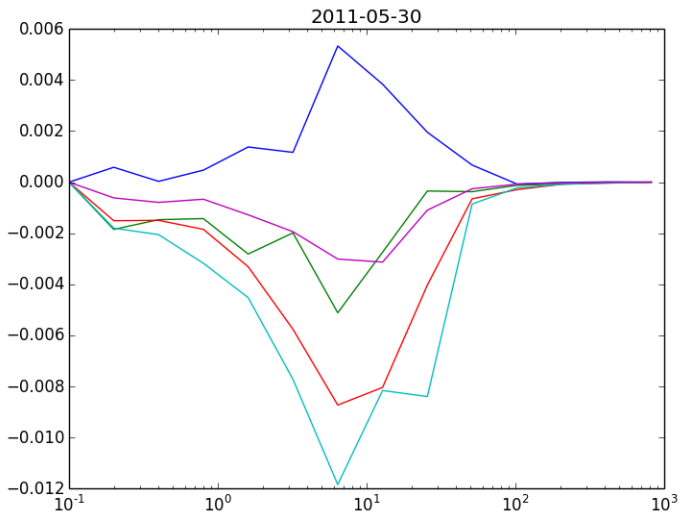

Figure 2.4: *The multi-resolutional decomposition found the gap on May 30, 2011 from 1800-2100. The average of all 5 hours is 53.76 seconds.*

The differences between these two gaps can be accounted for by looking at the average wind speed for those two time frames. The average wind speed for May 27, 2011 was slightly higher than the average wind speed for May 30, 2011, confirming that a different gap scale is needed in the same environment based on difference timeframes. On May 30, 2011, one of the lines also appears to have a heat flux in the opposite directions. This is the first of the 30 minute averages, and although the heat flux is in the opposite directions (possibly due to the sun still setting/ radiation differences) the gap that is found using the MRD will not be affected because it is taking the average of all of the gaps found and the gap appears to be on the same time frame as the other 30 minute periods.

D. IDENTIFYING TREE MOTION

Like all physical structures, trees have a natural mode of frequency and are susceptible to resonant loading. Therefore, understanding their periodic motion is fundamental to understanding the absorption and dissipation of wind energy (Rudnicki et al, 2008). Several studies have combined spectra from measurements of wind gusts with spectra characterizing tree sway in order to construct mechanical transfer functions. These types of studies reveal that wind gusts at or near the tree's natural sway frequency are efficiently transformed into tree motion and may induce resonance (Gardiner 1992; White et al.1976).

The Fourier transform method takes advantage of the fact that continuous signals can be decomposed to a sum of weighted sinusoidal functions. A Fast Fourier Transform (FFT) can be applied to each tree to detect the fundamental mode of frequency over the course of a particular time period. In previous studies the dominant frequency from each Fourier transformed data segment were identified by applying a cutoff of any frequency below 0.2 Hz and then automatically selecting the frequency with the highest power. The resulting frequencies are assumed to represent the fundamental mode of tree vibration. In this study an FFT was performed for each time segment identified by the MRD. That is for every 18.5 seconds of tree data for the first day that was picked a single FFT was computed. The frequency with the highest power was taken as the tree vibration due to turbulence. This process effectively creates a time series of frequency values for each tree.

In previous studies (Rudnicki et al. 2008), smoothing functions were used to find an interpretable result. In Rudnicki's study (2008) a Daniell filter was used for all of the trees to minimize leakage and retain detail (Bloomfield 2000). A Daniell filter is a smoothing process for displacement data, which helps to identify fundamental frequencies. However, while the Daniell filter was useful for spectral loss, when applying it to the sway data in this experiment, small changes in frequency from time step to time step were lost. This is likely because of the short time periods that are being examined in this experiment. Because this study is not only examining the fundamental frequencies of the trees, but rather the changes in frequency, the Daniell filter was not used. Instead a simple 5-point moving averaged was applied to the fourier power spectra to aid in automated identification of the fundamental frequency in each time step. All time series calculations, including the MRD and FFT were made using Python version 2.6 on a desktop PC. All the code can be found in Appendix A.

E. DYNAMIC MAPPING

In order to visualize how the fundamental frequency of each individual tree was changing over time, the change in frequency was mapped and categorized based on either an increase or a decrease in frequency. The study area was plotted according to exact latitude and longitude coordinates into a layer in ArcMap. The frequency data was imported into ESRI's ArcMap and "joined" to the tree layer based on the tree id number, which attached each frequency change in the time step to a particular location in space.

Once the data was geolocated a spatial interpolation was preformed for each time step (every 18.56 seconds for the first day and every 53.76 seconds for the second day). This turns the 149 individual time series of frequency changes into a series of maps. The analysis was done by batching all of the information for each tree and time period together and running the Natural Neighbor interpolation to give a complete picture of the entire data area.

The Natural Neighbor method is a geometric estimation technique that uses natural neighborhood regions generated around each point in the data set. Like the inverse distance weighting (IDW), this interpolation method is a weighted-average interpolation method. However, instead of finding an interpolated point's value using all of the input points weighted by their distance, Natural Neighbors interpolation creates a Delauney Triangulation of the input points and selects the closest nodes that form a convex hull around the interpolation point. It then “weighs” their values by proportionate area. This method is most appropriate where sample data points are distributed with uneven density. It is a good general-purpose interpolation technique and has the advantage that you do not have to specify parameters such as radius, number of neighbors or weights. This technique is designed to honor local minimum and maximum values in the point file and can be set to limit overshoots of local high values and undershoots of local low values. The method thereby allows the creation of accurate surface models from data sets that are very sparsely distributed or very linear in spatial distribution.

CHAPTER 3: RESULTS

Figure 3.1 shows an example of the process of converting tree displacement to changes in frequency. The figure shows the raw time signal and the FFT for trees # 75 and #76. Both are located near the center of the plot. By looking at the figure it can be observed that the chosen time scale for this particular night finds a change in for the onset and offset of gusts.

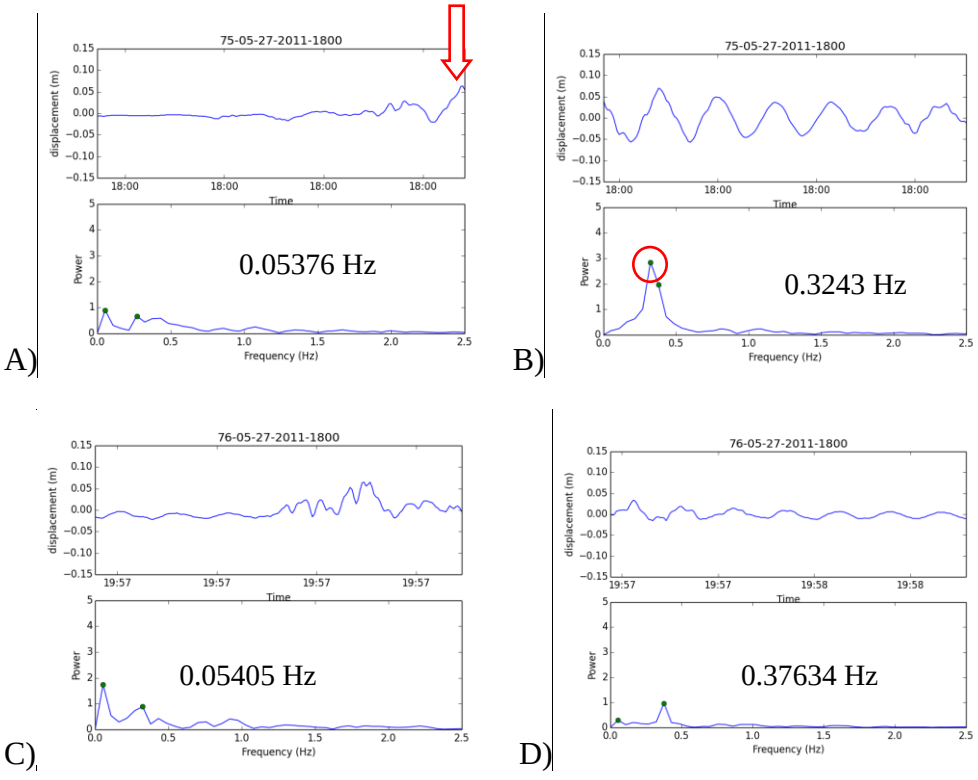

Figure 3.1: *FFT Results May 27, 2011 -- The purpose of comparing these two variables is to identify the onset of a gust in the forest (indicated by the arrow in Figure 3.1A) and then observe what happens to the peak frequency of that time frame(circled in Figure 3.1B) when the displacement is changing. Each top panel shows the displacement over a period of time. The bottom panels show the corresponding frequency change (power)—*

both on the x-axis. The peak frequency in the lower panel is denoted by a dot. The change in this peak frequency is the mapable variable for the animations. A&B Tree 75 from 18:00:00.01 to 18:00:37.22 C&D Tree 76 from 19:57:00.01 50 19:57:37.22

Figure 3.1 clearly indicated that there is a change in the tree's peak frequency upon the arrival of a gust. In *Figures 3.1A and 3.1B* it can be observed that the peak frequency of the tree is increased from 0.05Hz to 0.32Hz with the onset and occurrence of a gust. The same is true in Figures *3.1C and 3.1D,* which show the tree movement and frequency for a time later in the evening. Here the frequency changes from its resting level of 0.05Hz to a movement frequency of 0.37Hz. This indicates that a positive change in frequency is a good parameter for the identification of a gust affecting a tree in the forest. This was further analyzed to see if the apparent increase in the fundamental frequency does not just occur in one place, at one tree, but rather in groups, which can be identified throughout the study area.

In order to identify coherency at the MRD calculated time step, the FFT was also performed at another record length, which is double that of the spectral gap calculated using MRD. This was done as a control comparison. For May 27, 2011 this was a record length of 37 seconds and for May 30, 2011 a record length of 106 seconds was used. The output of the longer time FFT was also mapped using the same steps mentioned above. *Figure 3.2* shows the results for the same starting time presented in *Figure 3.1*. Thus, the left panels of *Figure 3.2* show the combined time series of panels A&B of *Figure 3.1* and the right panel shows the next 106 seconds. When the record time is doubled the figures show the fundamental or natural vibration frequency of the tree rather than the influence

of a gust (Webb et al, 1980), like the gap scale figures previously showed. This was true for the majority of the plots at the longer time length.

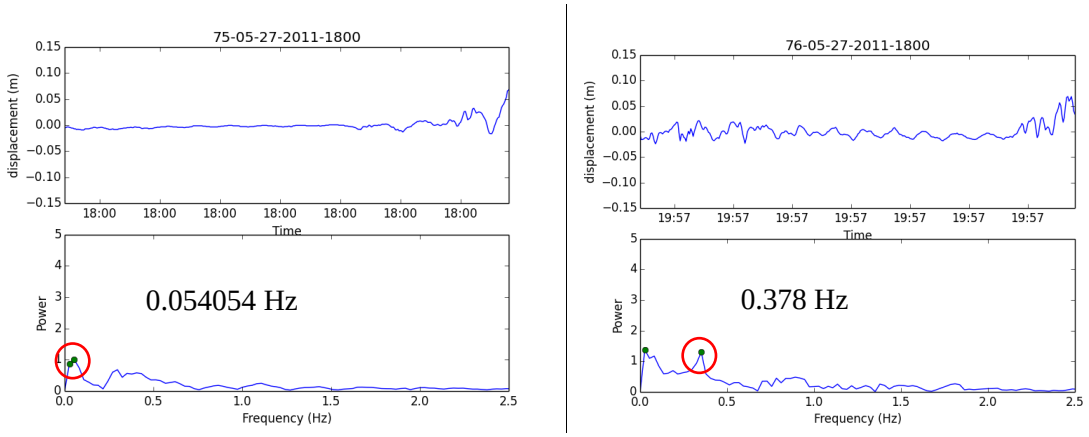

Figure 3.2: *FFT Results May 27, 2011—<u>double</u> record length. The left panel shows the combined time series of the top panels of Figure 3.1 and the right panel shows the combined time series of the bottom panels of Figure 3.1. Tree 75 is from 18:00:00.01 to 18:00:37.22 and Tree 76 is from 19:57:00.01 50 19:57:37.22. As the Red circles indicate, there is no detection of a peak frequency in these examples.*

Because the main goal of this thesis was to determine coherency in the data, only a subset of each night was mapped for visual aid. For each night the first 30 minutes of data was compiled into an animated map. This captures the occurrence of a moderate to high wind speed on each day, which as previously discussed, should yield more apparent gusts. Viewing of the animations, revealed an interesting picture of the forest. The animations are attached on an included CD. Static images from the animations are shown below for discussion. In all of the maps, shades of blue represent a decreasing change in frequency from the previous time step and the shades of red indicate an increase in frequency.

When observing the animations the movement of the gusts through the forest site becomes more apparent—particularly at the gap time scale. As shown in the static images, there are some instances in the time frame that I examined where a gust impression was apparent and a gust moved through the site, but it only appeared at the gap time scale animation and was completely missed, or virtually non-existent in the longer time step animation. The color changes between a decrease in frequency (blue) and an increase in frequency (reds) are usually very well coordinated—if there was a major increase as a gust moved through a section of a forest in one frame in the next frame there is a corresponding decrease in frequency as the tree begins to return back to its natural frequency. Overall movement in the animations corresponds with the wind direction observed by the central tower on the research site.

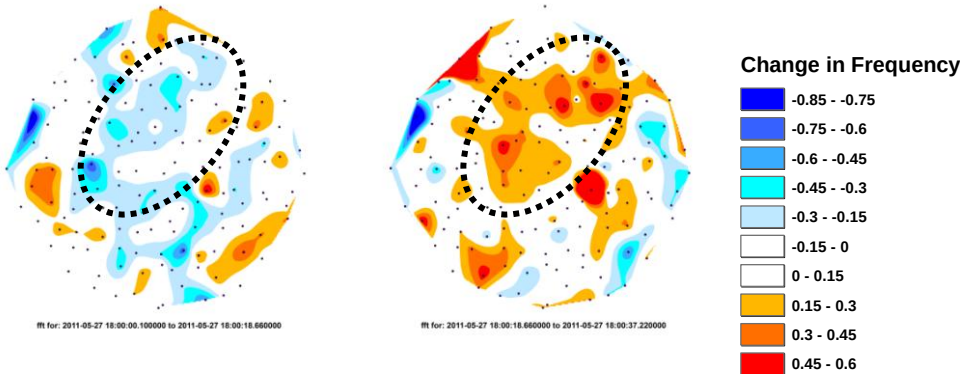

Figure 3.3: *Static images of the frequency changes occurring from 2011-05-27 18:00:00.01 to 18:00:37.22 at the gap time scale. During this time wind direction was predominantly from the northwest. Each image represents the frequency found from an 18 second record*

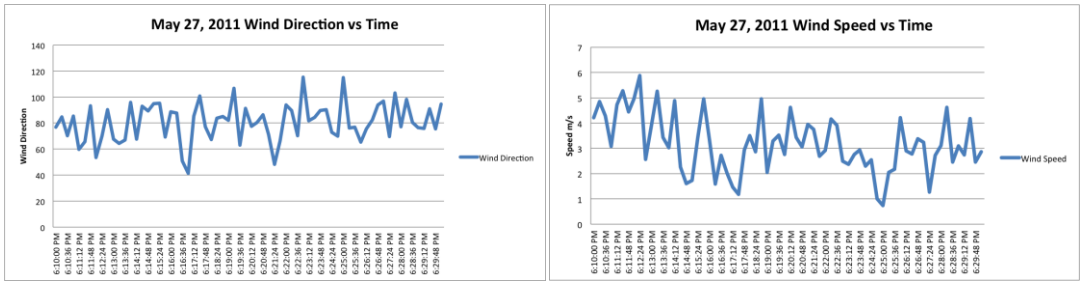

Figure 3.4: *Plots of the Wind Direction and Wind Speed corresponding with the time periods looked at in the attached animations.*

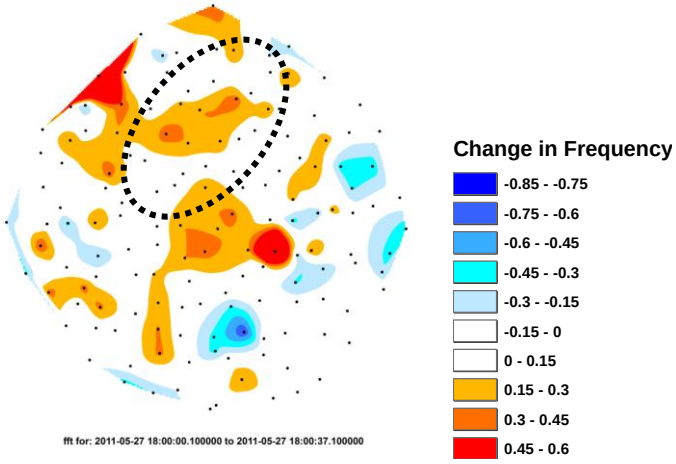

Figure 3.5: *Static image of the frequency changes occurring from 2011-05-27 18:00:00.01 to 18:00:37.22 at <u>double</u> the gap time scale.*

Figure 3.3 shows results from May 27th when computing frequency changes at the gap-scale. In the first image, a predominant decrease in frequency is seen through the center of the plot (highlighted with the dashed circle), with some areas of increase on the outer edges. In the second image a predominant increase in frequency is seen—which can be attributed to a response to the previous decrease in the time step before. This momentary decrease is interpreted as a gust moving the canopy. The wind speed shown in *Figure 3.4* confirms this. *Figure 3.5* shows the results of the computed frequency

changes at double the gap-scale on May 27th, 2011. The absence of any frequency increase or decrease indicates that the frequency changes are lost when computing frequency at times longer than the gap-scale. The decrease and subsequent increase in frequency would not have been detected and instead, the data would have just showed an overall decrease between those two time steps. Essentially, the tree's response to the gust occurring at the time is lost, and the bounce back, return to normalcy, or increase in frequency is not detected at double the gap scale.

A second example from May 27th is shown in Figure 3.6 below.

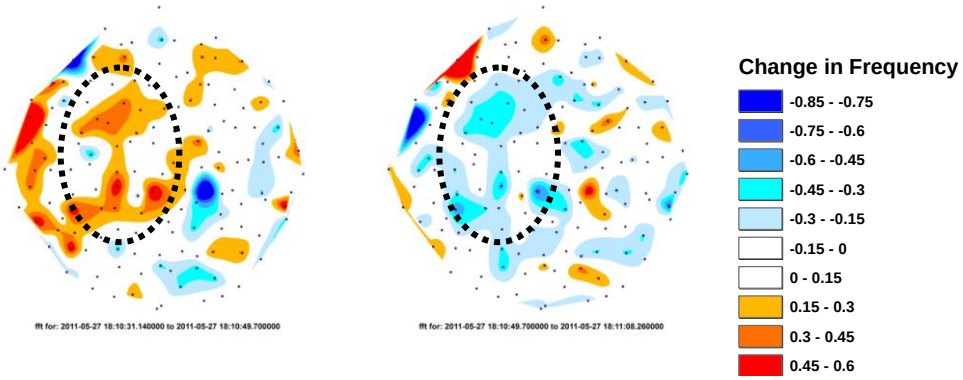

Figure 3.6*: Static images of the frequency changes occurring from 2011-05-27 18:10:31.14 to 18:11:08.26 at the gap time scale*

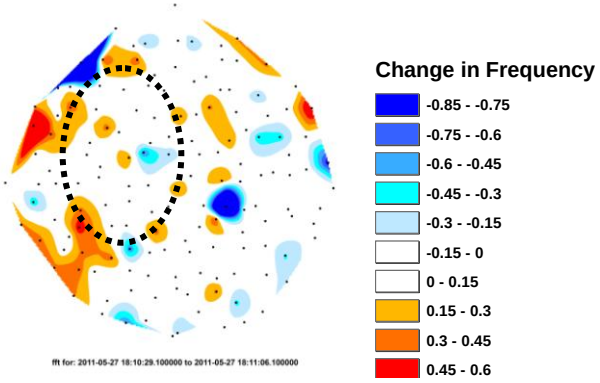

Figure 3.7: *Static image of the frequency change occurring from 2011-05-27 18:10:29.14 to 18:11:06.26 at <u>double</u> the gap time scale*

In the first two images above, there is an apparent gust impression occurring between the time steps of 18:10:31.14- 18:10:49.7 and 18:10:49:7- 18:11:08:26, however no gust is identifiable in *Figure 3.7*, which shows the computed frequency change when using double the gap-scale for the computation window. This is expected and apparent because of the theory proposed above that the gusts and coherent motions will be more visible at a time scale that is determined by MRD, rather than an averaged time scale for the entire study time.

On the night of May 30th, the wind speed was 2.4m/s and the gap-scale was longer (53.76 seconds). Overall the results are similar with more coherency and subtle changes in tree motion seen when using the proposed gap-scale as a window-length versus a longer period. *Figure 3.8* below shows several static images from this night. These images are interesting because even though the average wind speed for this night was slightly slower than the previous date chosen, coherent motions can still clearly be seen at

the gap scale and are completely overlooked at the double time step (highlighted with dashed circle). This indicates that choosing an appropriate time scale for these gusts is even more important when the wind speed is not as high.

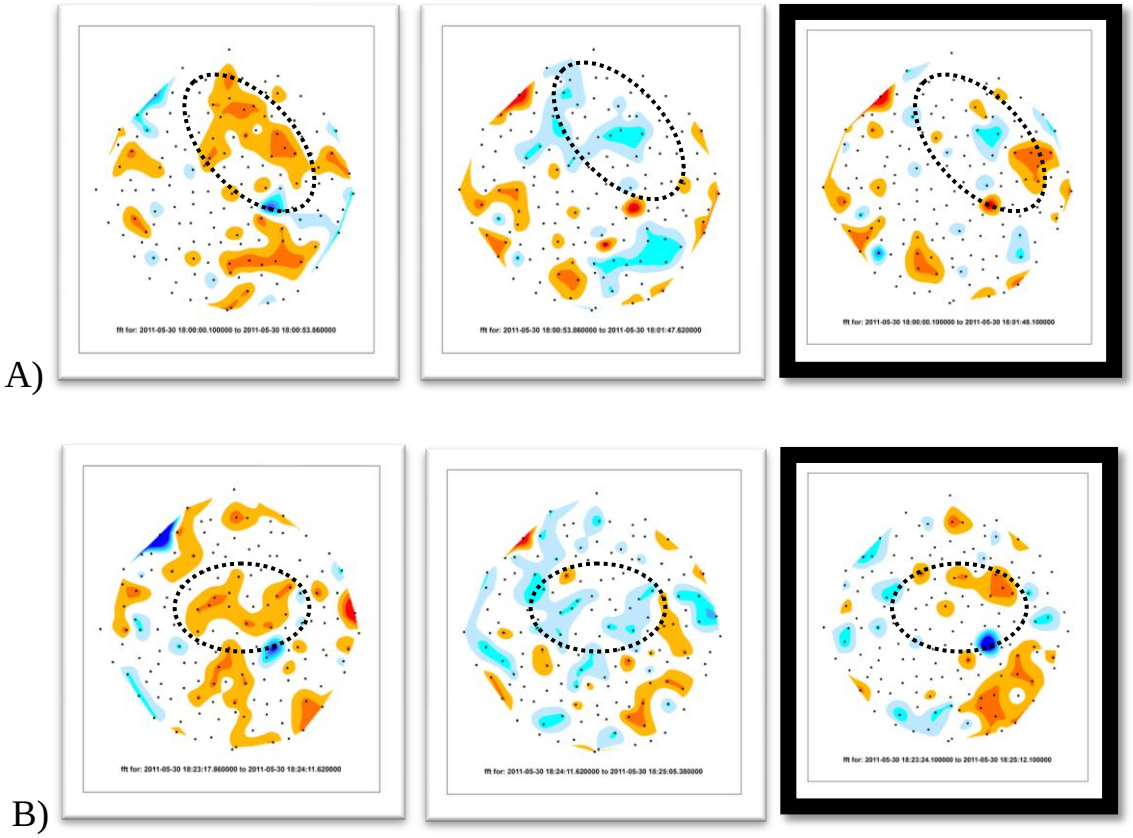

Figure 3.8: *(A) Static images of the frequency changes occurring from 2011-05-30 18:00:00.01 to 18:01:47.62 at the gap time scale with the outlined image showing the same time frame, but double the gap time scale (B) Static images of the frequency changes occurring from 2011-05-30 18:23:17.86 to 18:25:05.38 at the gap time scale with the outlined image showing the same time frame, but double the gap time scale*

CHAPTER 4: DISCUSSION/ CONCLUSION

The results presented in chapter three confirm the original hypothesis that coherent motions in a forest canopy are occurring on turbulent time scales. Less coherence is seen when examining motion on time scales greater than the co-spectral gap, which would include meso and sub meso scale motions. This further proves that identifying the importance of a time scale is imperative to predicting the response of trees in a forest environment. In this particular case, frequency proved to be a good variable for mapping the wind and capturing the occurrence of the small-scale gusts. Overall this work highlights how helpful dynamic maps can be for displaying rapidly changing spatial patterns. As a preliminary analysis this work also highlights a number of other future research directions.

Several aspects of this study could be improved in the future. When looking back at the mapping outputs, a particular tree is always highlighted. After looking more into the specifics of this tree it is clear that it is much bigger than the surrounding trees, hence causing the FFT to highlight it more often. This could also have something to do with the method of peak detection algorithm that was chosen—another method might have been better or more accurate. Also, more standardization of the data might have prevented this. Also, because of the limitations of this study, only two days out of several years of data were used. Expanding the time frame would have given us a better look at the differences eddy movement associated with the different weather conditions and seasons. It also, still

remains unclear as to whether this method will work for moderate wind speed days, when the changes in frequency are not as noticeable, as only days with high winds speeds were chosen for this particular study.

The animations that were created for this project were a great start, but there needs to be more flexibility in controlling the time step as well as the time frame that can be looked at. If the time step could be customized and changed to start later in the time frame it would ensure that any gust, at any point in the forest can be captured. This means that you could track the movement of a gust from its entrance to the research site until it exits—still using the gap scale. If a tool like this could be created, it would help to apply these findings to other areas, not just forests so that researchers can get an idea of how small-scale winds interact on a variety of different terrains.

The more immediate take away from this study pertains to the specific field of micrometeorology and forestry. Now that I have proved that there is coherency occurring in the boundary layer at particular time scales, the next step is to figure out what can define this coherency and how to move forward into defining exactly what constitutes as spatial correlation, i.e. a certain number of trees moving in the same direction, etc. Identifying areas that are spatially correlated would help in forestry management/damage predictions.

There has long been an underlying assumption in meteorology that sub synoptic-scale phenomena such as turbulence might be responsible for the difficulty in making quality weather forecasts beyond a few days. Therefore, part of the effort in boundary layer

meteorology involves the search for accurate turbulence parameterization schemes for larger-scale numerical forecast models. Progress made from this project will build a foundation, in both field experimental design and numerical model development, for pursuing investigations of these interactions in more complex situations in the near future.

REFERENCES

Amiro, B. D. "Comparison of Turbulence Statistics Within Three Boreal Forest Canopies." *Boundary-Layer Meteorology* 51, no. 1–2 (April 1, 1990): 99–121. doi:10.1007/BF00120463.

Baker, C.J. "The Development of a Theoretical Model for the Windthrow of Plants." *Journal of Theoretical Biology* 175, no. 3 (August 7, 1995): 355–372. doi:10.1006/jtbi.1995.0147.

Baldocchi, D. D. & Hutchinson, B. A. 1987 Turbulence in an almond orchard: vertical variation in turbulence statistics. Boundary-Layer Meteorol. 40, 177–146.

Baldocchi, Dennis D., and Tilden P. Meyers. "Turbulence Structure in a Deciduous Forest." *Boundary-Layer Meteorology* 43, no. 4 (June 1, 1988): 345–364. doi:10.1007/BF00121712.

Banta, R., R. Newsom, J. Lundquist, Y. L. Pichugina, R. L. Coulter,and L. Mahrt, 2002: Nocturnal low-level jet characteristics over Kansas during CASES-99.Bound.-Layer Meteor., 105, 221–252.

Bloomfield P (2000) Fourier analysis of time series: an introduction. Wiley, New York

Bohm, M., Finnigan, J. J. & Raupach, M. R. 2000 Dispersive fluxes and canopy flows: just how important are they? In Proceedings of 24th Conference on Agricultural and Forest Meteorology, American Meteorological Society, Davis, CA.

Boose, Emery R., David R. Foster, and Marcheterre Fluet. "Hurricane Impacts to Tropical and Temperate Forest Landscapes." *Ecological Monographs* 64, no. 4 (November 1994): 369. doi:10.2307/2937142.

Brunet, Y., J. J. Finnigan, and M. R. Raupach. "A Wind Tunnel Study of Air Flow in Waving Wheat: Single-point Velocity Statistics." *Boundary-Layer Meteorology* 70, no. 1–2 (July 1, 1994): 95–132. doi:10.1007/BF00712525.

Businger, J. A., J. C. Wyngaard, Y. zumi, and E. F. Bradley, 1971:Flux profile relationships in the atmospheric surface layer. J.Atmos. Sci., 28, 181–189.

Canham and Loucks 1984 Ecol 65 803 809 Pdf Free Ebook Download. Accessed April 8, 2013. http://ebookbrowse.com/canham-and-loucks-1984-ecol-65-803-809-pdf-d337224477.

Cellier, P., and Y. Brunet. “Flux-gradient Relationships Above Tall Plant Canopies.” *Agricultural and Forest Meteorology* 58, no. 1–2 (March 1992): 93–117. doi:10.1016/0168-1923(92)90113-I.

Colorado, Atmospheric Studies Program Area J. C. Kaimal Chief, Wave Propagation Laboratory Environmental Research Laboratories National Oceanic and Atmospheric Administration Boulder, and Center for Environmental Mechanics J. J. Finnigan Head, Australia National Oceanic and Atmospheric Administration Boulder Colorado. *Atmospheric Boundary Layer Flows : Their Structure and Measurement: Their Structure and Measurement*. Oxford University Press, 1993.

Dale, V. H., L. A. Joyce, S. McNulty, R. P. Neilson, M. P. Ayres, M. D. Flannigan, P. J. Hanson, et al. *Climate Change and Forest Disturbances*, 2001. http://www.treesearch.fs.fed.us/pubs/30125.

David Foster, and Emery R. Boose. “Patterns of Forest Damage Resulting from Catastrophic Wind in Central New England, USA” (n.d.).

Dyer, A., 1974: A review of flux-profile relationships. Bound.-Layer Meteor., 7, 363–372.

Dwyer, M. J., Patton, E. G. & Shaw, R. H. 1997 Turbulent kinetic energy budgets from a large-eddy simulation of airflow above and within a forest. Boundary-Layer Meteorol. 84,23–43.

Emanuel, Kerry. “Increasing Destructiveness of Tropical Cyclones over the Past 30 Years.” *Nature* 436, no. 7051 (August 4, 2005): 686–688. doi:10.1038/nature03906.

Finnigan 2000 Annual Review Fluid Mech Pdf Free Ebook Download. Accessed April 8, 2013. http://ebookbrowse.com/finnigan-2000-annual-review-fluid-mech-pdf-d131921957.

Finnigan, John. “Turbulence in Plant Canopies.” *Annual Review of Fluid Mechanics* 32, no. 1 (2000): 519–571. doi:10.1146/annurev.fluid.32.1.519

———. “Turbulence in Plant Canopies.” *Annual Review of Fluid Mechanics* 32, no. 1 (2000): 519–571. doi:10.1146/annurev.fluid.32.1.519.

Gao, W., R. H. Shaw, and K. T. Paw U. “Observation of Organized Structure in Turbulent Flow Within and Above a Forest Canopy.” In *Boundary Layer Studies and Applications*, edited by R. E. Munn, 349–377. Springer Netherlands, 1989. http://link.springer.com/chapter/10.1007/978-94-009-0975-5_22.

Gardiner B (1992) Mathematical modelling of the static and dynamic characteristics of plantation trees. In: Franke J, Roeder A (eds) Mathematical modelling of forest ecosystems. Sauerlander, Frankfurt, pp 40–61

Gardiner, B. A. "Wind and Wind Forces in a Plantation Spruce Forest." *Boundary-Layer Meteorology* 67, no. 1–2 (January 1, 1994): 161–186. doi:10.1007/BF00705512.

Henry, Hugh A. L., and Sean C. Thomas. "Interactive Effects of Lateral Shade and Wind on Stem Allometry, Biomass Allocation, and Mechanical Stability in Abutilon Theophrasti (Malvaceae)." *American Journal of Botany* 89, no. 10 (October 1, 2002): 1609–1615. doi:10.3732/ajb.89.10.1609.

Howell, J. F., and L. Mahrt, 1997: Multiresolution flux decomposition.Bound.-Layer Meteor., 83, 117–137

Irvine, M. R., B. A. Gardiner, and M. K. Hill. "The Evolution Of Turbulence Across A Forest Edge." *Boundary-Layer Meteorology* 84, no. 3 (September 1, 1997): 467–496. doi:10.1023/A:1000453031036.

James, Kenneth R, Nicholas Haritos, and Peter K Ades. "Mechanical Stability of Trees Under Dynamic Loads." *American Journal of Botany* 93, no. 10 (October 2006): 1522–1530. doi:10.3732/ajb.93.10.1522.

Kaimal, J. C., and J. J. Finnigan, 1994: Atmospheric Boundary Layer Flows: Their Structure and Measurements. Oxford University Press, 289 pp.

Katul, G G, A Porporato, R Nathan, M Siqueira, M B Soons, D Poggi, H S Horn, and S A Levin. "Mechanistic Analytical Models for Long-distance Seed Dispersal by Wind." *The American Naturalist* 166, no. 3 (September 2005): 368–381. doi:10.1086/432589.

Katul, G., and B. Vidakovic, 1996: The partitioning of attached and detached eddy motion in the atmospheric surface layer using Lorentz wavelet filtering. Bound.-Layer Meteor., 77, 153–172.

Law, Beverly. "Carbon Dynamics in Response to Climate and Disturbance: Recent Progress from Multi-scale Measurements and Modeling in AmeriFlux" (n.d.).

Mahrt, L., 1998: Flux sampling strategy for aircraft and tower observations. J. Atmos. And Oceanic Technol., 15, 416-429.

Marshall, B. J., C. J. Wood, B. A. Gardiner, and R. E. Belcher. "Conditional Sampling Of Forest Canopy Gusts." *Boundary-Layer Meteorology* 102, no. 2 (February 1, 2002): 225–251. doi:10.1023/A:1013181714844.

Milne, R. "Dynamics of Swaying of Picea Sitchensis." *Tree Physiology* 9, no. 3 (October 1, 1991): 383–399. doi:10.1093/treephys/9.3.383.

Monsi, M, Z Uchijima, and T Oikawa. “Structure of Foliage Canopies and Photosynthesis.” *Annual Review of Ecology and Systematics* 4, no. 1 (1973): 301–327. doi:10.1146/annurev.es.04.110173.001505.

Monteith, J. L. “Climatic Variation and the Growth of Crops.” *Quarterly Journal of the Royal Meteorological Society* 107, no. 454 (1981): 749–774. doi:10.1002/qj.49710745402.

Mulhearn, P. J., and J. J. Finnigan. “Turbulent Flow over a Very Rough, Random Surface.” *Boundary-Layer Meteorology* 15, no. 1 (August 1, 1978): 109–132. doi:10.1007/BF00165509.

Peterson, C J. “Catastrophic Wind Damage to North American Forests and the Potential Impact of Climate Change.” *The Science of the Total Environment* 262, no. 3 (November 15, 2000): 287–311.

Porter, John R., and Mikhail A. Semenov. “Crop Responses to Climatic Variation.” *Philosophical Transactions of the Royal Society B: Biological Sciences* 360, no. 1463 (November 29, 2005): 2021–2035. doi:10.1098/rstb.2005.1752.

Py, Charlotte, Emmanuel De Langre, and Bruno Moulia. “A Frequency Lock-in Mechanism in the Interaction Between Wind and Crop Canopies.” *Journal of Fluid Mechanics* 568 (2006): 425–449. doi:10.1017/S0022112006002667.

Py, Charlotte, Emmanuel de Langre, Bruno Moulia, and Pascal Hémon. “Measurement of Wind-induced Motion of Crop Canopies from Digital Video Images.” *Agricultural and Forest Meteorology* 130, no. 3–4 (June 30, 2005): 223–236. doi:10.1016/j.agrformet.2005.03.008.

Raupach, M R, and A S Thom. “Turbulence in and Above Plant Canopies.” *Annual Review of Fluid Mechanics* 13, no. 1 (1981): 97–129. doi:10.1146/annurev.fl.13.010181.000525.

Raupach, M. R., J. J. Finnigan, and Y. Brunei. “Coherent Eddies and Turbulence in Vegetation Canopies: The Mixing-layer Analogy.” *Boundary-Layer Meteorology* 78, no. 3–4 (March 1, 1996): 351–382. doi:10.1007/BF00120941.

Raupach, M. R., H. Mayer, W. Kohsiek, B. Gardiner, J. A. Clarke, R. Amtmann, J. M. Crowther, P. G. Jarvis, and R. Milne. “Windthrow: Discussion.” *Royal Society of London Philosophical Transactions Series B* 324 (August 1, 1989): 279–281.

Raupach, M. R., and R. H. Shaw. “Averaging Procedures for Flow Within Vegetation Canopies.” *Boundary-Layer Meteorology* 22, no. 1 (January 1, 1982): 79–90. doi:10.1007/BF00128057.

Rudnicki, Mark, Stephen J Mitchell, and Michael D Novak. “Wind Tunnel Measurements of Crown Streamlining and Drag Relationships for Three Conifer

Species." *Canadian Journal of Forest Research* 34, no. 3 (March 2004): 666–676. doi:10.1139/x03-233.

Shaw, Roger H., and Ulrich Schumann. "Large-eddy Simulation of Turbulent Flow Above and Within a Forest." *Boundary-Layer Meteorology* 61, no. 1–2 (October 1, 1992): 47–64. doi:10.1007/BF02033994.

Speck, Olga, and Hanns-Christof Spatz. "Damped Oscillations of the Giant Reed Arundo Donax (Poaceae)." *American Journal of Botany* 91, no. 6 (June 1, 2004): 789–796. doi:10.3732/ajb.91.6.789.

SpringerLink (Online service), and European Science Foundation. *Forest Diversity and Function Temperate and Boreal Systems*. Edited by M. Scherer-Lorenzen, Christian Körner, and E.-D. Schulze. Ecological Studies v. 176. Berlin ; New York: Springer, 2005. http://library.sc.edu/catalog/off campus.html?url=http://dx.doi.org/10.1007/b137862.

Stull, R. B., 1990: An Introduction to Boundary Layer Meteorology. Kluwer Academic, 666 pp.

Telewski, Frank W., and Michele L. Pruyn. "Thigmomorphogenesis: a Dose Response to Flexing in Ulmus Americana Seedlings." *Tree Physiology* 18, no. 1 (January 1, 1998): 65–68. doi:10.1093/treephys/18.1.65.

Thomas, Christoph, and Thomas Foken. "Flux Contribution of Coherent Structures and Its Implications for the Exchange of Energy and Matter in a Tall Spruce Canopy." *Boundary-Layer Meteorology* 123, no. 2 (May 1, 2007): 317–337. doi:10.1007/s10546-006-9144-7.

Trapp. "Changes in Severe Thunderstorm Environment Frequency During the 21st Century Caused by Anthropogenically Enhanced Global Radiative Forcing." *Proceedings of the National Academy of Sciences of the United States of America* 104, no. 50 (2007): 19719–19723. doi:DOI 10.1073/pnas.0705494104.

Vickers, D., and L. Mahrt, 1997: Quality control and flux sampling problems for tower and aircraft data. J. Atmos. Oceanic Technol.,14, 512–526.

Vickers, Dean, and L. Mahrt. "A Solution for Flux Contamination by Mesoscale Motions With Very Weak Turbulence." *Boundary-Layer Meteorology* 118, no. 3 (March 1, 2006): 431–447. doi:10.1007/s10546-005-9003-y.

Watanabe, Masahiro. "Asian Jet Waveguide and a Downstream Extension of the North Atlantic Oscillation." *Journal of Climate* 17, no. 24 (December 2004): 4674–4691. doi:10.1175/JCLI-3228.1.

Watanabe, Tsutomu. “Large-Eddy Simulation of Coherent Turbulence Structures Associated with Scalar Ramps Over Plant Canopies.” *Boundary-Layer Meteorology* 112, no. 2 (August 1, 2004): 307–341. doi:10.1023/B:BOUN.0000027912.84492.54.

White RG, White MF, Mayhead GJ (1976) Measurement of the motion of trees in two dimensions. Technical report no. 86. Institute of Sound and Vibration Research, University of Southhampton

Wilson, N. Robert, and Roger H. Shaw. “A Higher Order Closure Model for Canopy Flow.” *Journal of Applied Meteorology* 16, no. 11 (November 1977): 1197–1205. doi:10.1175/1520-0450(1977)016<1197:AHOCMF>2.0.CO;2.

White RG, White MF, Mayhead GJ (1976) Measurement of the motion of trees in two dimensions. Technical report no. 86. Institute of Sound and Vibration Research, University of Southhampton

APPENDIX A – PYTHON CODE

MRD_OneFile.py

```
import glob, os from numpy import * from multires import * import
matplotlib.pylab as plt from datetime import datetime from datetime import date
from time_functions import *

# open all data

path='/THESIS_030414/ThesisData/WindData/'

file1 = path+'2011-05-27-1800.txt' # this is where you change the file names
avg_time=30 # this is the base averaging time to determine turbulent
components

##### read the first file print "current file is: " + file1 data1 =
genfromtxt(file1, delimiter=',', names=True, autostrip=True, dtype=None) #
read the data

# check data

if bitwise_or((data1['diag_csat_below'].max() > 63),
(data1['diag_csat_below'].min() < print ' results from the bottom sonic on: ',
file1, 'should be ignored due to errors in the sonic data'

exit()

if bitwise_or((data1['diag_csat_middle'].max() > 63),
(data1['diag_csat_middle'].min() <

print ' results from the middle sonic on: ', file1, 'should be ignored due to
errors in the sonic data'

exit()

if bitwise_or((data1['diag_csat_top'].max() > 63),
(data1['diag_csat_top'].min() < 0)):

print ' results from: ', file1, 'should be ignored due to errors in the sonic
data'

exit()

# join them
```

```
temptimes=concatenate([data1['TIMESTAMP']])
wind_dict={'u_top':concatenate([data1['u_top']]),
'v_top':concatenate([data1['v_top']]),

'w_top':concatenate([data1['w_top']]),
'Ts_top':concatenate([data1['Ts_top']]),
'u_mid':concatenate([data1['u_middle']]),
'v_mid':concatenate([data1['v_middle']]),
'w_mid':concatenate([data1['w_middle']]),
'Ts_mid':concatenate([data1['Ts_middle']]),
'u_bot':concatenate([data1['u_below']]),
'v_bot':concatenate([data1['v_below']]),
'w_bot':concatenate([data1['w_below']]),
'Ts_bot':concatenate([data1['Ts_below']])}

numrecords=len(temptimes)

print "there are", numrecords, 'records'

# change timestamps to python date time timestamp = []

for i in range(0, numrecords):

if len(temptimes[i]) < 22: timestamp.append(datetime.strptime(temptimes[i],
'"%Y-%m-%d %H:%M:%S"'))

else: timestamp.append(datetime.strptime(temptimes[i], '"%Y-%m-%d
%H:%M:%S.%f"')) filedate=date(timestamp[0].year, timestamp[0].month,
timestamp[0].day) u = wind_dict['u_top'] w = wind_dict['w_top'] T =
wind_dict['Ts_top']

wprime=getprimes(w,timestamp,avg_time) Tprime=getprimes(T,timestamp,avg_time)

# run MRD

 print "beginning MRD calculations" mrd_results = mrd_9000(u, wprime, Tprime,
temptimes, 10, 0.5)

# find the gap for each MRD

print "finding average gapscale" num_of_mrds=len(mrd_results['results'][0])
gaps_first=zeros(num_of_mrds) gaps_level=zeros(num_of_mrds)
gaps_after_min=zeros(num_of_mrds) times=mrd_results['time_scale']
```

```
print times count=0 while count < num_of_mrds: # for each mrd
values=mrd_results['results'][:,count] low_peak=min(values)
low_peak_index=where(values == low_peak)

for step in range(0,len(times)-1):

# find first increase after a decrease "gaps_first"

if mrd_results['results'][step+1,count] > mrd_results['results'][step,count]:
gaps_first[count]=times[step+1] break for step in range(0,len(times)-1):

#check that change is > 1% of total flux accum_flux=sum(values[0:step+1])
current_accum_flux=sum(values[0:step+2]) one_percent_change=0.01*accum_flux

if current_accum_flux-accum_flux > one_percent_change:
gaps_level[count]=times[step+1] break for step in
range(low_peak_index[0],len(times)-1):

 #find the first increase after the low peak

if mrd_results['results'][step+1,count] > mrd_results['results'][step,count]:
gaps_after_min[count]=times[step+1] break count=count+1

print 'gaps after first decrease ='

print gaps_first print 'gaps after minium peak ='

print gaps_after_min print 'gaps where flux levels ='

print gaps_level

#setup output

outfile = open("gaps"+str(filedate)+".txt", "w")

outfile.write("first increase, first increase after min, gap at level off\n")
outfile.write(str(mean(gaps_first))+","+str(mean(gaps_after_min))+','+str(mean
(gaps_level)))

outfile.close()

#=============================================================================
= # fig=plt.figure(i) ax=fig.add_subplot(1,1,1)
ax.plot(mrd_results['time_scale'],mrd_results['results']) ax.set_xscale('log')
ax.set_title(filedate) plt.savefig(str(filedate)+'.jpg') plt.show()
```

```
#=============================================================================
= # write output file print "program complete"
```

Multires.py

```
# example IDL driver program #a = [ 1., 3., 2., 5., 1., 2., 1., 3. ] #b = a
#M=3 #D=multires(a,b,M) #print,'D(m),m=1,M ',D

# ---- multiresolution decomposition ---- ;

def multires(a, b, m): import numpy as np n_params = 3 d = np.zeros(m) ims=m
for ims in np.arange(m, 0,-1): l = 2.0 ** ims nw = (2.0 ** m) / l sumab = 0.0
for i in np.arange(0,nw): k = (i - 1) * l + 1 za = a[k - 1] zb = b[k - 1] for
j in np.arange(k, (k + l)): za = za + a[j - 1] zb = zb + b[j - 1] za = za / l
zb = zb / l sumab = sumab + za * zb for j in np.arange(k, (i * l)): a[j - 1] =
a[j - 1] - za b[j - 1] = b[j - 1] - zb if (nw > 1): d[ims] = (sumab / nw)
return d

def mrd_9000(u, w, T, timestamp, sample_rate, total_period): import numpy as
np import math as math from scipy.interpolate import interp1d

# total_period should be input in hours # sample rate should be in hertz

#-----------------------------------------

#constants n_params = 3 delta_t = 1.0/sample_rate

#determining length of mrd

num_secs = total_period * 3600.

# determine sample length (needs to be a power of two)

n = num_secs * sample_rate

#total length of the recored to run mrd on

num_segs = np.floor(len(u)/n)

#number of mrds to run on the whole data record

m = np.floor(math.log10(n) / math.log10(2))

#number of points to map to to be a even power of two #reassign N so samples
are run sequentially

 n = 2.0 ** m
```

```
# define the averaging periods that will be used and initialize the output
array

values = np.zeros([m, num_segs]) averaging_periods = np.arange(0,m)
averaging_periods = (2.0 ** averaging_periods) * delta_t i = 0

#for each subset for i in np.arange(0,num_segs):

#Map to 2^M data points new_delta_t = (n - 1) * delta_t / ((2.0 ** m) - 1)
new_points = np.arange(0,2.0 ** (m)) * new_delta_t mapped_w =
interp1d(w[(i*n):(i*n)+n], new_points) mapped_T=interp1d(T[(i*n):(i*n)+n],
new_points)

#perform the MRD values[:,i] = multires(mapped_w.x, mapped_T.x, m)

print 'mrd performed for', 2.0 ** m, 'data points'

print 'initial data rate is', delta_t

print 'start time of data', timestamp[i*n]

print 'stop time of data', timestamp[(i*n)+n]
output={'time_scale':averaging_periods,'results':values}

print 'mrd calculations complete'

return output
```

TreeFFT.py

```
import os

import numpy as np

import datetime as dt

import matplotlib.pyplot as plt from scipy.signal

import argrelmax from peakdetect

import * from math

import * from Daniell

import *

def movingaverage(interval, window_size): window=
np.ones(int(window_size))/float(window_size) return np.convolve(interval,
window, 'same')

avg_time=18.56 # this will be the averaging time found from the mrd plots_on =
'y' #set to 'n' to suppress creation of plots (suggested for short averaging
periods)

# read a file output_path='/Users/kertell/Desktop/FFTData/Output/TEST/'
filename='/Users/kertell/Desktop/FFTData/Fast-XYinM-05-27-2011-1800.dat'

print "current file is: " + filename data = np.genfromtxt(filename,
delimiter=',', names=True, dtype=None, autostrip=True) # read the data
numrecords = len(data) # number of lines in input file print "numrecords is " +
str(numrecords) print "file reading complete, converting timestamps..."
################################################################ # change
timestamps to python date time timestamp = [] for i in range(0, numrecords):
rawtime=data['Datemmddyear'][i]+' '+data['Timehrminmillisec'][i].replace('
','') timestamp.append(dt.datetime.strptime(rawtime, '%m-%d-%Y %H:%M:%S.%f'))
print "timestamps converted, beginning calculations..." flist =
os.path.basename(filename) name_only = flist[11:-4] print name_only
output_file=open(output_path+name_only+'_fft_peak1.dat', 'w')
output_file2=open(output_path+name_only+'_fft_peak2.dat','w')
output_file.write('fft calculations computed for every '+str(avg_time)+'
seconds\n') output_file2.write('fft calculations computed for every
'+str(avg_time)+' seconds\n')

################################################################
```

```
# # iterate for the number of columns

for col in range(2,len(data.dtype.names)-15,2): sensorx=data.dtype.names[col]
sensory=data.dtype.names[col+1] print 'computing fft for:', sensorx, sensory
#calculate displacement disp=np.sqrt(data[sensorx]**2+data[sensory]**2)

# subset the data

total_length=timestamp[len(timestamp)-1]-timestamp[0]
number_periods=int(total_length.seconds/avg_time) period_start=timestamp[0]
period_start_times=[] peak1=[sensorx[1:]] peak2=[sensorx[1:]]

for i in range(0,number_periods): new_data=[]
period_start_times.append(period_start)

# times are the start time for each average period
period_end=period_start+dt.timedelta(0,avg_time)

# calculate the end time for each average period

for index, item in enumerate(timestamp):

if item <= period_start: start_index=index

if item <= period_end: stop_index=index

if (stop_index-start_index) < 1: new_data.append(float('nan')) print 'no fft
found for:', period_start, 'to', period_end

else: new_data.append(disp[start_index:stop_index]) print 'finding fft for:',
period_start, 'to', period_end

#output_file.write('peak frequencies for sensor '+str(sensorx[1:])+' beginning
at '+str(period_start)+' and ending at '+str(period_end)+'\n')

# removal of mean

new_data=new_data[0]-(sum(new_data[0])/len(new_data[0]))

# subtract the mean
windspeed=np.sqrt(data['Utop'][start_index:stop_index]**2+data['Vtop'][start_i
ndex:stop_index]** mean_windspeed=sum(windspeed)/len(windspeed)

#compute the fft

ps_raw=np.abs(np.fft.fft(new_data))

freq_raw=np.fft.fftfreq(stop_index-start_index, d=0.1)
```

```
# smooth it -- standard moving average over 10 points
ps=movingaverage(ps_raw[0:(len(ps_raw)/2)-1], 1)
freq=freq_raw[0:(len(ps_raw)/2)-1]

#----no smooth -------- ps=ps_raw[0:(len(ps_raw)/2)-1]
freq=freq_raw[0:(len(ps_raw)/2)-1] #------

#OPTION 3 ------- just find the biggest value --------------------
peakpower_index=np.argsort(ps)[::-1][:len(ps)]
peakfreq=freq[peakpower_index[0:2]] peakpower=ps[peakpower_index[0:2]]
peak1.append(freq[peakpower_index[0]]) peak2.append(freq[peakpower_index[1]])
if plots_on == 'y':

# plot plt.figure(1) rawplot=plt.subplot(211)
rawplot.plot(timestamp[start_index:stop_index],new_data)

import matplotlib.dates as mdates

myFmt = mdates.DateFormatter('%H:%M')

rawplot.xaxis.set_major_formatter(myFmt)

rawplot.set_xlabel('Time')

rawplot.set_ylabel('displacement (m)')

rawplot.set_ylim([-0.15,0.15])

rawplot.set_title(sensorx[1:]+'-'+name_only)

fftplot=plt.subplot(212)

fftplot.plot(freq,ps)

fftplot.plot(peakfreq,peakpower,'o')
#fftplot.plot(peakfreq[top_index[0:3]],peakpower[top_index[0:3]],'*')
fftplot.set_xlabel('Frequency (Hz)')

fftplot.set_ylabel('Power')

fftplot.set_xlim([0,2.5])

fftplot.set_ylim([0,5])

fftplot.text(0.6,15,'mean windspeed:'+str(round(mean_windspeed,2)))

print 'mean_windpseed:', mean_windspeed
```

```
print output_path+sensorx+name_only[:-4]+str(int(start_index/10))
plt.savefig(output_path+sensorx[1:]+'-'+name_only+'-'+str(i))

plt.show()

plt.close()

plt.clf()

period_start=period_end

# update to the start of the next period

output_file.write(str(peak1))

 output_file.write('\n')

output_file2.write(str(peak2))

output_file2.write('\n')

output_file.close()

output_file2.close()

print 'program complete'
```